we suggest that the direct addition of $Cr(ClO_4)_2$ to **1** leads to the rapid two one-electron reduction of the quinone ring to give the bis-Cr^{III}-bound complex **12** (Scheme II).[17] Loss of methanol then yields **13**, which allows the C-1 and C-10 *nucleophilic substitution processes to proceed by an indole-assisted pathway*.[18] The corresponding electrophilic transformations should be inhibited by the prior complexation of the phenolic-type oxygens at C-5 and C-8 in **12** and **13** by the chromium ion. The high yields of the C-1, C-10 disubstituted adducts **3** and **5** have been attributed to the full two-electron reduction of **1** to species **12** (**13** and **14**). We suspect that the corresponding indole-assisted expulsion of the C-10 carbamate group at the semiquinone stage would not proceed rapidly due to the electron deficiency of this species.

This study documents the advantages accrued by the direct use of $Cr(ClO_4)_2$ for the reductive activation of mitomycin C. Reactions were rapid and permitted the functionalization of both DNA bonding sites within **1**. Our attribution of the high percentage of nucleophilic products in these transformations to the complexation of the C-5 and C-8 phenolic-type oxygens in **12** by the metal raises the intriguing suggestion that a similar process (i.e., protonation, hydrogen-bonding, chelation) may be necessary for the full expression of drug function of reduced **1** in in vivo transformations.

Acknowledgment. We thank the National Institutes of Health (RO1CA29756) and the Robert A. Welch Foundation (E607) for their generous support of our work. Grateful acknowledgment is made to Dr. A. M. Casazza and Bristol-Myers Laboratories, Wallingford, CT, for a generous gift of mitomycin C. Special thanks are given to Professor Thomas Albright for many helpful discussions.

(17) Analysis of the HPLC profiles indicated that a minor fraction of the products under acidic conditions may arise from an autocatalytic pathway in which a chromium bound mitomycin C species serves as a chemical reductant for **1**.

(18) Addition of $Cr(ClO_4)_2$ to buffered *methanolic* solutions of **1** led to high yields of *cis*- and *trans*-10-decarbamoyl-1,10-dimethoxymitosene. Analogously, addition of $Cr(ClO_4)_2$ (1 equiv) to aqueous buffered (pH 6.00) solutions of **2** and **4** gave principally **3** and **5**, respectively.[19]

(19) Hong, Y. P.; Kohn, H. Unpublished results.

Formation of Monolayer Pits of Controlled Nanometer Size on Highly Oriented Pyrolytic Graphite by Gasification Reactions As Studied by Scanning Tunneling Microscopy

Hsiangpin Chang and Allen J. Bard*

Department of Chemistry
The University of Texas at Austin
Austin, Texas 78712

Received January 22, 1990

We report here that nanometer-size pits with monolayer depth are reproducibly formed on the basal (0001) plane of highly oriented pyrolytic graphite (HOPG) by gasification reactions at elevated temperature in air. These are clearly imaged and easily studied by scanning tunneling microscopy (STM).

Gas–carbon reactions are important in studies of combustion, water gas production, and the gasification of solid fuels.[1] Progress in this area has largely depended upon the application of microscopic techniques, from optical microscopy to the more powerful etch-decoration transmission electron microscopy (ED-TEM)[2-4] or scanning electron microscopy (ED-SEM).[5] In ED-TEM a graphite sample etched by reaction with O_2, CO_2, H_2O, H_2, or Cl_2 is decorated with evaporated gold which nucleates at the etched edges, allowing surface changes to be imaged by electron microscopy. Etch decoration with gold is needed because clear images of unmodified carbon surfaces are not obtained by TEM. Studies by ED-TEM[2-4] on natural graphite led to a model in which monolayer pits form during gasification reactions. These were proposed to start at existing defects (e.g., atomic vacancies) and grow in a shape determined by the higher reactivity of carbon atoms at edge sites. However, it was not possible to study by EM the initial stages of this process on unmodified graphite or to show that these etch pits are one atomic layer deep.[2a]

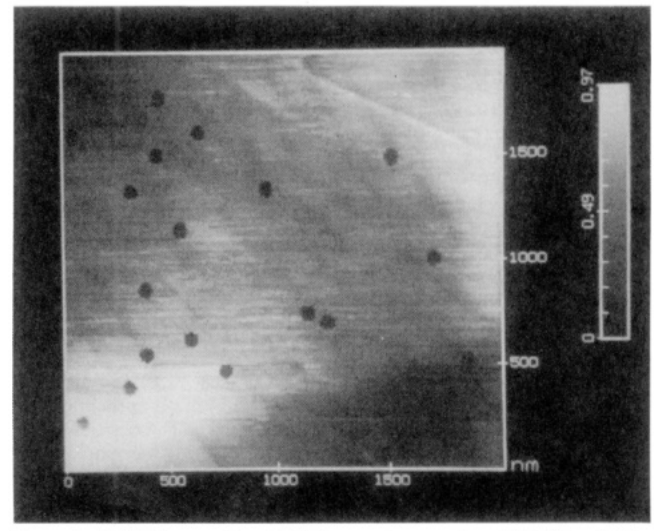

Figure 1. STM image of an HOPG sample treated at 650 °C in air for 15 min.

However, STM[6] allows surface imaging with atomic resolution on graphite surfaces. We felt that STM could be used to image etch pits, without the requirement of gold decoration, from the initial stages of their formation. We are interested in these pits not only because they provide information about the mechanism of carbon oxidation but also because pits of a controlled and uniform size could have interesting applications as templates and markers. In this work HOPG,[7] rather than the related natural graphite crystals used in earlier investigations,[2a] was studied. The oxidation of HOPG has not been investigated by high-resolution electron microscopy.[8]

(1) (a) Kinoshita, K. *Carbon: Electrochemical and Physical Properties*; Wiley: New York, 1988; Chapter 4. (b) Thomas, J. M. In *Chemistry and Physics of Carbon*; Walker, P. L., Jr., Ed.; Marcel Dekker: New York, 1965; Vol. 1, pp 122–203. (c) Strange, J. F.; Walker, P. L., Jr. *Carbon* **1976**, *14*, 345. (d) McKee, D. W. *ibid.* **1970**, *8*, 623. (e) Laine, N. R.; Vastola, F. J.; Walker, P. L. *J. Phys. Chem.* **1963**, *67*, 2030. (f) Bonner, F.; Turkevich, J. *J. Am. Chem. Soc.* **1951**, *73*, 561. (g) Lewis, W. K.; Gilliland, E. R.; McBride, G. T., Jr. *Ind. Eng. Chem.* **1949**, *41*, 1213.

(2) (a) Yang, R. T. In *Chemistry and Physics of Carbon*; Walker, P. L., Jr., Thrower, P. A., Eds.; Marcel Dekker: New York, 1984; Vol. 19, pp 163–210. (b) Hennig, G. R. *ibid.*; Walker, P. L., Jr., Ed.; 1966; Vol. 2, pp 1–50. (c) Baker, R. T. K. *Catal. Rev.-Sci. Eng.* **1979**, *19*, 161.

(3) (a) Yang, K. L.; Yang, R. T. *AIChE J.* **1985**, *31*, 1313. (b) Yang, R. T.; Yang, K. L. *Carbon* **1985**, *23*, 537. (c) Duan, R.-Z.; Yang, R. T. *Chem. Eng. Sci.* **1984**, *39*, 795. (d) Yang, R. T.; Wong, C. *J. Catal.* **1984**, *85*, 154. (e) Yang, R. T.; Wong, C. *Science* **1981**, *214*, 437. (f) Yang, R. T.; Wong, C. *AIChE J.* **1983**, *29*, 338.

(4) (a) Hennig, G. R. *J. Chem. Phys.* **1964**, *40*, 2877. (b) Hennig, G. R. *J. Inorg. Nucl. Chem.* **1962**, *24*, 1129. (c) Evans, E. L.; Griffiths, R. J. M.; Thomas, J. M. *Science* **1970**, *171*, 174. (d) Feates, F. S. *Trans. Faraday Soc.* **1968**, *64*, 3093. (e) Montet, G. L.; Myers, G. E. *Carbon* **1968**, *6*, 627.

(5) (a) Wong, C.; Yang, R. T. *J. Chem. Phys.* **1983**, *78*, 3325. (b) Wong, C.; Yang, R. T. *Ind. Eng. Chem. Fund.* **1983**, *22*, 380. (c) Yang, R. T.; Wong, C. *Rev. Sci. Instrum.* **1982**, *53*, 1488.

(6) (a) Binnig, G.; Rohrer, H. *Helv. Phys. Acta* **1982**, *55*, 726. (b) Binnig, G.; Rohrer, H.; Gerber, Ch.; Weibel, E. *Phys Rev. Lett.* **1982**, *49*, 57. (c) Binnig, G.; Rohrer, H. *IBM J. Res. Develop.* **1986**, *30*, 355. (d) Hansma, P.; Tersoff, J. *J. Appl. Phys.* **1987**, *61*, R1.

(7) HOPG was generously supplied by Arthur W. Moore of Union Carbide Corporation, Parma, OH. The samples were cleaved with either sticky tape or a razor before oxidation.

(8) (a) Rodriguez-Reinoso, F.; Thrower, P. A.; Walker, P. L., Jr. *Carbon* **1974**, *12*, 63. (b) Rodriguez-Reinoso, F.; Thrower, P. A. *Carbon* **1974**, *12*, 269. (c) Rellick, G. S.; Thrower, P. A.; Walker, P. L., Jr. *Carbon* **1975**, *13*, 71.

0002-7863/90/1512-4598$02.50/0

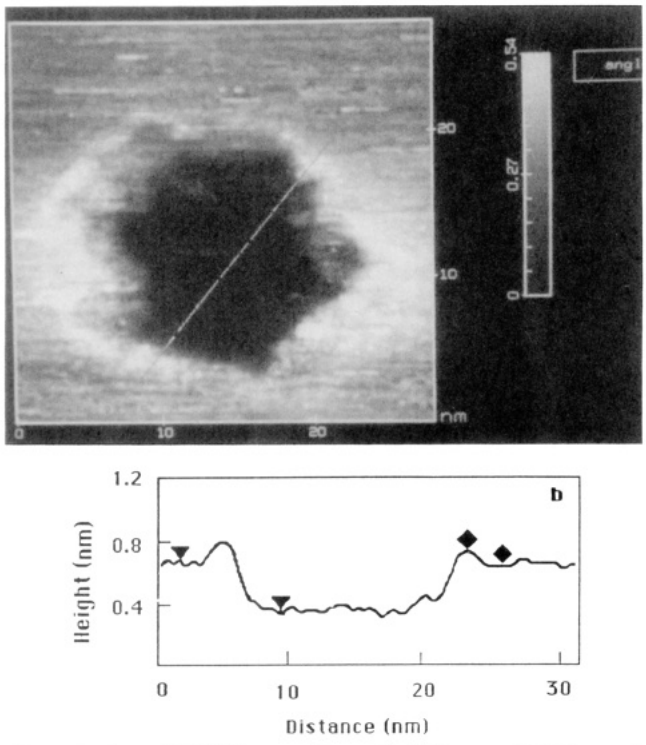

Figure 2. (a, top) STM image of an etch pit from an HOPG sample treated at 650 °C in air for 5 min. (b, bottom) Depth profile along the line shown in part a. The height difference between the markers is (▼) 3.5 Å and (◆) 1.2 Å.

Shown in Figure 1 is a typical STM image[9] of etch pits on an HOPG sample treated at 650 °C in air[10] for 15 min. These pits formed at a given time were quite uniform in size and shape. The relative standard deviation of the diameter values is smaller than 10%. The uniform size of the pits indicates that they are initiated at the same time on naturally occurring vacancies on HOPG, rather than on vacancies formed during the oxidation, which occurs only at higher temperatures.[2-4] The average vacancy density on HOPG, obtained from inspection of more than 30 images of 4 different samples, is $3.1 \pm 1.5\ \mu m^{-2}$, which is smaller than those values reported for natural graphite.[2,3] Besides the regular pits shown in Figure 1, a much smaller number of pits and channels with irregular shapes were sometimes observed. These are probably due to initiation and growth at impurities (e.g., small dust particles) on the HOPG surface, since we have observed large numbers of similar structures on HOPG samples that were treated with NaCl, CrO_3, H_2PtCl_6, and many other particulate materials.

The detailed structure of the edges of the pits can be seen by STM. A single pit formed at 650 °C for 5 min is shown in Figure 2a. The depth of the etch pits can be easily measured from the STM height profile,[11] as shown in Figure 2b. The averaged value is 3.4 ± 0.2 Å, which is exactly the spacing between graphite layers (3.35 Å). Therefore, these etch pits are indeed one atom deep. This material may thus be useful in the *z*-axis calibration of an STM. Multilayer pits were also sometimes observed, and their depths were multiples of 3.4 Å. These multilayer pits probably occur when a vacancy at the second layer is exposed during the growth of a pit on the first layer. A 20–30-Å region around the edges of the pits is different from that in the smooth regions on the basal planes between and at the bottom of the pits. This appears on the profile in Figure 2b as a slightly raised (ca. 1.2 Å) region. This could represent an actual upward displacement of carbon atoms at the edge or a change in the tunneling barrier height in this region. A similar edge structure was observed on cleavage steps on freshly cleaved HOPG[12] and on holes generated on HOPG by a voltage pulse at an STM tip.[13] The usual atomic structure of graphite could be imaged both inside and outside of the pits, away from the edges, suggesting that the oxidation of the top graphite layer leaves the underlayer intact. However, atomic resolution was difficult to achieve on the edges.

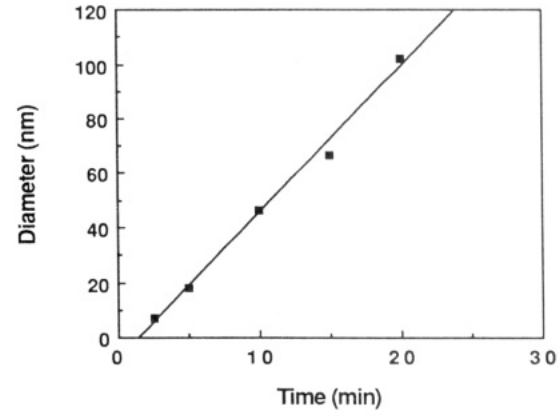

Figure 3. Diameter of the etch pits as a function of reaction time at 650 °C.

The diameter of the pits[14] increased linearly with reaction time when the reaction temperature was kept constant at 650 °C, as shown in Figure 3. A similar relation was observed for much larger etch pits with ED-TEM.[2-4] This curve, whose slope is 5.2 nm/min, can be used as a calibration for the pit sizes. The smallest pit observed on a sample heated for 2.5 min has a diameter of 5 nm. Pits larger than 500 nm were observed on a sample heated for over 1 h. The linear growth of the pit diameter can be understood in terms of a linear increase with time in the number of reactive carbon sites on a single pit during oxidation. The shape of the pits also changed with reaction time. Pits larger than 200 nm were usually circular, which is consistent with the ED-TEM results.[2-4] However, most of the pits in the 40–200-nm range have a more hexagonal shape, as shown in Figure 2a. Pits smaller than 40 Å had irregular shapes.

In conclusion, we have demonstrated that monolayer etch pits of a controllable size over the entire surface of HOPG are reproducibly generated by gasification reactions. This technique is more effective in generating pits on HOPG surfaces than other existing techniques, e.g., by STM fabrication with short voltage pulses.[13] Clearly STM is a powerful technique for studying the early stages of the gasification of graphite and observing the nanometer scale features generated by the reactions. These etch pits may have several applications. For example, they may be useful as templates for the synthesis of species, such as ultra-small semiconductor particles, as markers for STM imaging, and as active sites for HOPG surface modification in chemically modified electrodes and for immobilization of molecules for STM imaging. Future studies might also include the study of gasification reactions at other temperatures and pressures, in the presence of catalysts, and with oxidants other than dioxygen.

Acknowledgment. The support of the Texas Advanced Research Program is gratefully acknowledged.

(9) A NanoScope II STM (Digital Instruments, Santa Barbara, CA) was used. Pt–Ir (80:20) microtips (Digital Instruments) were used following electrochemical etching as described in: Gewirth, A. A.; Craston, D. H.; Bard A. *J. Electroanal. Chem.* **1989**, *261*, 477. Both images are in height mode without any filtering. The images usually did not change with imaging parameters, including bias voltage (±300 mV), setpoint current (0.7–2 nA), and scan rate (2–8 Hz).

(10) A Lindberg tube furnace (Watertown, WI) was used for heating. The HOPG sample was placed in a porcelain crucible. Heating was started by placing the crucible with sample into the furnace preheated to the desired temperature. The sample was cooled by withdrawing it from the furnace into the air.

(11) The depth of the pits was measured repeatedly from the depth profile instead of point-to-point comparison to avoid false measurement due to the increased noise and sample tilting at the edges. Smoothing the image with lowpass filtering, which does not alter the depth of the pits, was found necessary to obtain the depth profile with least noise.

(12) Chang, H.; Bard, A. J. In preparation.

(13) Albrecht, T. R.; Dovek, M. M.; Kirk, M. D.; Lang, C. A.; Quate, C. F.; Smith, D. P. E. *Appl. Phys. Lett.* **1989**, *55*, 23.

(14) These diameter values are the averaged results from measurement of over 50 pits for each reaction time. The diameter for each pit was measured repeatedly in different directions.